REPORT

Cell Cycle 11:7, 1383-1392; April 1, 2012; © 2012 Landes Bioscience

Oncogene-induced senescence results in marked metabolic and bioenergetic alterations

Celia Quijano,[1,2] Liu Cao,[1] Maria M. Fergusson,[1] Hector Romero,[3] Jie Liu,[1] Sarah Gutkind,[1] Ilsa I. Rovira,[1] Robert P. Mohney,[4] Edward D. Karoly[4] and Toren Finkel[1,*]

[1]Center for Molecular Medicine; National Heart Lung and Blood Institute; National Institutes of Health; Bethesda, MD USA; [2]Departamento de Bioquímica; Facultad de Medicina; Universidad de la República; Montevideo, Uruguay; [3]Laboratorio de Organización y Evolución del Genoma; Facultad de Ciencias/C.U.R.E.; Universidad de la República; Montevideo, Uruguay; [4]Metabolon Incorporated; Research Triangle Park, NC USA

Key words: oncogene-induced senescence, metabolomics, Ras, fatty acid oxidation

Oncogene-induced senescence (OIS) is characterized by permanent growth arrest and the acquisition of a secretory, pro-inflammatory state. Increasingly, OIS is viewed as an important barrier to tumorgenesis. Surprisingly, relatively little is known about the metabolic changes that accompany and therefore may contribute to OIS. Here, we have performed a metabolomic and bioenergetic analysis of Ras-induced senescence. Profiling approximately 300 different intracellular metabolites reveals that cells that have undergone OIS develop a unique metabolic signature that differs markedly from cells undergoing replicative senescence. A number of lipid metabolites appear uniquely increased in OIS cells, including a marked increase in the level of certain intracellular long chain fatty acids. Functional studies reveal that this alteration in the metabolome reflects substantial changes in overall lipid metabolism. In particular, Ras-induced senescent cells manifest a decline in lipid synthesis and a significant increase in fatty acid oxidation. Increased fatty acid oxidation results in an unexpectedly high rate of basal oxygen consumption in cells that have undergone OIS. Pharmacological or genetic inhibition of carnitine palmitoyltransferase 1, the rate-limiting step in mitochondrial fatty acid oxidation, restores a pre-senescent metabolic rate and, surprisingly, selectively inhibits the secretory, pro-inflammatory state that accompanies OIS. Thus, Ras-induced senescent cells demonstrate profound alterations in their metabolic and bioenergetic profiles, particularly with regards to the levels, synthesis and oxidation of free fatty acids. Furthermore, the inflammatory phenotype that accompanies OIS appears to be related to these underlying changes in cellular metabolism.

Introduction

Senescence is a state of irreversible growth arrest that can be triggered by a wide range of cellular stresses. Historically, senescence was first characterized in the context of the limited proliferative capacity of primary human cells in culture.[1] Subsequent studies have demonstrated that the growth arrest that occurs following serial passaging of human cells, termed replicative senescence, results from an erosion in telomere length.[2,3] Telomere attrition, in turn, generates a persistent DNA damage response (DDR) that appears to be required to enforce the growth-arrested state.[4] Other stresses besides passage-dependent telomere shortening can also induce senescence. Perhaps the best-studied examples come from conditions that directly induce DNA damage (e.g., reactive oxygen species, X-rays or certain drugs) or situations in which cells experience strong and continuous mitogenic signals. One well-characterized example of the latter form of senescence is obtained following expression of the Ras oncogene in primary cells.[5] In many ways, senescence triggered by Ras expression or replicative stress is similar, with both forms of senescence resulting in cells exhibiting characteristic morphological changes, permanent growth arrest, persistent DDR activation as well as biochemical changes that include senescence-associated β-galactosidase expression (SA-β-Gal).

Increasing evidence suggests that OIS, as typified by oncogenic Ras expression, represents an important in vivo barrier to prevent tumor formation. Numerous animal models have established that strong oncogenic stimulation generates OIS within the premalignant lesions observed in these models, while senescent cells are absent from the tumors that ultimately emerge.[6,7] Similar observations have also been made in human tissues, where, for example, OIS cells are evident in premalignant melanocytic nevi but absent in malignant melanoma.[8] Likewise, other models have demonstrated that in addition to oncogene expression, loss of tumor suppressor function can also trigger OIS.[9] Taken together, these results solidify the notion that OIS represents an important functional checkpoint constraining malignant transformation.

While OIS cells are growth-arrested, a growing body of evidence suggests that these cells are far from inert. Indeed, senescent cells appear to develop a highly active secretory phenotype characterized by robust production of various inflammatory cytokines.[10,11] The expression of these various inflammatory mediators appears to reinforce aspects of the senescent state. Analyses

*Correspondence to: Toren Finkel; Email: finkelt@nih.gov
Submitted: 02/22/12; Accepted: 02/22/12
http://dx.doi.org/10.4161/cc.19800

using various models have implicated insulin-like growth factor-binding protein 7,[12] interleukin-6[13] and the chemokine receptor 2 (CXCR2) and its cognate ligands IL-8 and GROα[14] in the development and/or maintenance of OIS. In addition, this secretory and pro-inflammatory milieu has been implicated as a contributor to various age-related deficits, including impaired tissue repair and maintenance, altered stem cell function and tumor progression.[11,15,16] Indeed, many of the same cytokines found to be highly expressed by senescent cells in culture are also elevated in the serum of elderly individuals. Furthermore, levels of these cytokines appear to provide predictive power regarding the development of age-dependent frailty and overall mortality.[17-19]

Relatively little is known regarding the metabolic alterations that occur with the entry into senescence. Some reports have indicated that senescent fibroblasts exhibit a decrease in glycolysis.[20] Consistent with these observations, inhibition of glycolytic enzymes can induce senescence.[21] Similarly, replicative and OIS cells appear to have an increase in overall lipid content.[22,23] Finally, both replicative and oncogene-induced senescent cells have evidence of impaired mitochondrial function and increased oxidant formation.[24-26]

Here, we have performed a metabolic and bioenergetic analysis of Ras-induced senescence and demonstrate marked alterations particularly with regards to the levels, synthesis and oxidation of free fatty acids. Furthermore, the inflammatory phenotype that accompanies OIS appears to be in part related to these underlying changes in cellular metabolism.

Results

Metabolomic profile of oncogene-induced senescence. In order to more fully understand the mechanisms underlying OIS, we performed unbiased metabolic profiling of Ras-induced senescent human fibroblasts (**Fig. S1**). Cell lysates from six replicates per condition were obtained and analyzed using various mass spectrometry platforms. These platforms included gas chromatography (GC)-MS with electron ionization (EI) and liquid chromatography (LC)-MS/MS with electrospray ionization (ESI). This analysis allowed for the identification of 292 structurally named compounds, including metabolites found in a wide array of biochemical pathways, including amino acids, carbohydrates, lipids and nucleotides. Heatmap and hierarchical clustering by individual metabolites revealed that the metabolic profile of Ras-induced senescent cells appeared markedly distinct from uninfected early passage cells or from similar early passage cells infected with a control lentivirus (**Fig. 1A; Table S1**). Indeed, 155 out of 292 measured metabolites exhibited significant differences between Ras-infected vs. control-infected cells (cutoff for significance $p < 0.05$, Welch two sample t-test using q-values for False Discovery Rate estimation). These observed differences in the metabolome of the various cell groups may reflect dissimilarity in the metabolic profile of senescent vs. non-senescent cells or the inherent differences between growth-arrested OIS cells and replicating early passage uninfected or control-infected fibroblasts. Therefore, to further pursue this notion, we also analyzed the metabolome of cells that had undergone replicative senescence (**Fig. 1A**). Surprisingly, the metabolic profile of Ras-induced senescent cells and replicative senescent cells appeared to be clearly distinguishable from each other, with an even greater number of individual metabolites differing between these two seemingly similar senescent states (176 out of 292 measured metabolites exhibiting significant differences using the Welch two sample t-test; $p < 0.05$).

To further examine this phenomenon, we next employed the dimension reduction strategy of principal components analysis (PCA). In this approach, a large number of metabolic variables can be reduced into a smaller number of orthogonal variables (PC1, PC2, etc.) that capture the variation between our 24 separate samples. Using such analysis, we found that replicative senescent and Ras-induced senescent cells exhibited markedly distinct metabolomes (**Fig. 1B**).

We next sought to analyze those metabolites present in high abundance in Ras-induced senescent cells that were not similarly elevated in cells undergoing replicative senescence, control-infected early passage cells or uninfected early passage cells. We found 41 metabolites that were elevated by 2-fold or greater solely in Ras-induced senescent cells (**Fig. 2A; Table S2**). A smaller group of 21 metabolites were decreased 2-fold or more only in the OIS cells (**Fig. S2; Table S3**). Biochemical pathway analysis (e.g., amino acids, carbohydrates, lipids, nucleotides, etc.) demonstrated that more than half of the metabolites uniquely elevated in Ras-induced senescent cells were intracellular lipids (**Fig. 2B**). Particularly striking was an elevation of free fatty acids observed within OIS cells (**Fig. 2C**). Indeed, certain long-chain free fatty acids (FFA) appeared to be at roughly 5- to 10-fold higher concentrations in Ras-induced senescent cells (**Table S2**) when compared with the levels of these metabolites in either replicative senescent cells, uninfected early passage cells or early passage cells infected with a control lentivirus.

OIS cells exhibit alterations in lipid metabolism. The observed alterations in FFA suggested that cells undergoing OIS might manifest dynamic changes in overall lipid metabolism. Nonetheless, the observed alterations in FFA represent steady-state levels and are not helpful in determining the actual flux of fatty acid metabolites. One possible explanation for these observations would be a significant increase in de novo lipid synthesis in OIS cells. To directly address this hypothesis, we measured the level of ongoing lipid synthesis in control-infected or Ras-infected cells. To control for differences in proliferation, the experiments were performed with control-infected cells that had undergone confluent-dependent growth arrest and Ras-infected cells that had undergone senescent-dependent growth arrest. As seen in **Figure 3A**, we noted that there was in fact a decrease in lipid synthesis in Ras-infected cells both at day 8 (approximately 10% SA-β-Gal positive) and day 14 after infection (approximately 60–80% SA-β-Gal-positive). To explore the possible mechanism behind this observed decrease in lipid synthesis, we took advantage of previous observations that have established acetyl-CoA carboxylase 1 (ACC1) as the rate-limiting enzyme in fatty acid synthesis. These past studies have further demonstrated that the activity of ACC1 is negatively regulated by AMPK-dependent phosphorylation on a specific serine 79 residue.[27,28] Consistent with the observed decrease in lipid

synthesis, we observed an increase in the level of phosphorylated and hence inactive ACC1 in Ras-infected cells (**Fig. 3B**). As has been previously observed in reference 26, this was also accompanied by a concomitant increase in activated AMPK kinase in OIS cells (**Fig. 3B**).

In many situations, rates of fatty acid synthesis and fatty acid oxidation are inversely regulated due to the dual role of malonyl-CoA as a key substrate for fatty acid synthesis and a simultaneous inhibitor of carnitine palmitoyltransferase I (CPT1). As previously noted, CPT1 is the outer mitochondrial membrane protein that catalyzes the rate-limiting step in fatty acid oxidation. Consistent with this inverse regulation between lipid synthesis and fatty acid oxidation, we noted that compared with confluent-arrested control cells, Ras-induced senescent cells exhibited a marked elevation in fatty acid oxidation (**Fig. 3C**). Since some of the free fatty acids that were elevated in OIS cells, including molecules such as linoleate, palmitoleate and α-linolenate, are known to undergo oxidation in the mitochondria,[29,30] we next directly measured the rates of mitochondrial oxygen consumption in control-infected or Ras-infected human fibroblasts. We observed that Ras-infected cells exhibited a marked increase in basal oxygen consumption (**Fig. 3D**). This increase was not a result of any apparent change in mitochondrial uncoupling (**Fig. S3**). Treatment of Ras-infected cells with Etomoxir (ethyl 2-[6-(4-chlorophenoxy)hexyl]oxirane-2-carboxylate), a specific pharmacological inhibitor of CPT1 resulted in an acute decline in oxygen consumption. Similar pharmacological treatment of control early passage cells resulted in a much less dramatic effect on overall oxygen consumption, reflecting a reduced role of fatty acid oxidation in the basal metabolism of these cells (**Fig. 3D**). Indeed, the nearly 2-fold increase in mitochondrial oxygen consumption observed in Ras-induced senescent cells appeared entirely dependent on the observed increase in fatty acid oxidation (**Fig. 3E**). In contrast, we observed no marked differences in the basal respiration or fatty acid dependent oxygen consumption of cells that had undergone replicative senescence when they were compared with the respiration seen in early passage cells (**Fig. S4**).

Increased fatty acid oxidation regulates the secretory state of OIS cells. To further understand whether this alteration in fatty acid oxidation contributed to the phenotype of OIS cells, we simultaneously transduced human fibroblasts with both a Ras-expressing lentivirus and with lentiviral shRNAs that targeted CPT1A, a protein essential for the transport of FFA into the mitochondria. Two independent targeting constructs produced comparable knockdown of CPT1A expression (**Fig. 4A**). These targeting constructs produced comparable biological effects, and, as such, representative data from only one of these constructs is presented. As was observed with Etomoxir-treated cells, stable genetic inhibition of CPT1A reduced the oxygen consumption and hence basal metabolic rate of Ras-infected cells while having little effect on control cells (**Fig. 4B**). Again, this is compatible with the relative contribution of fatty acid oxidation in the basal metabolism of early passage control cells vs. cells

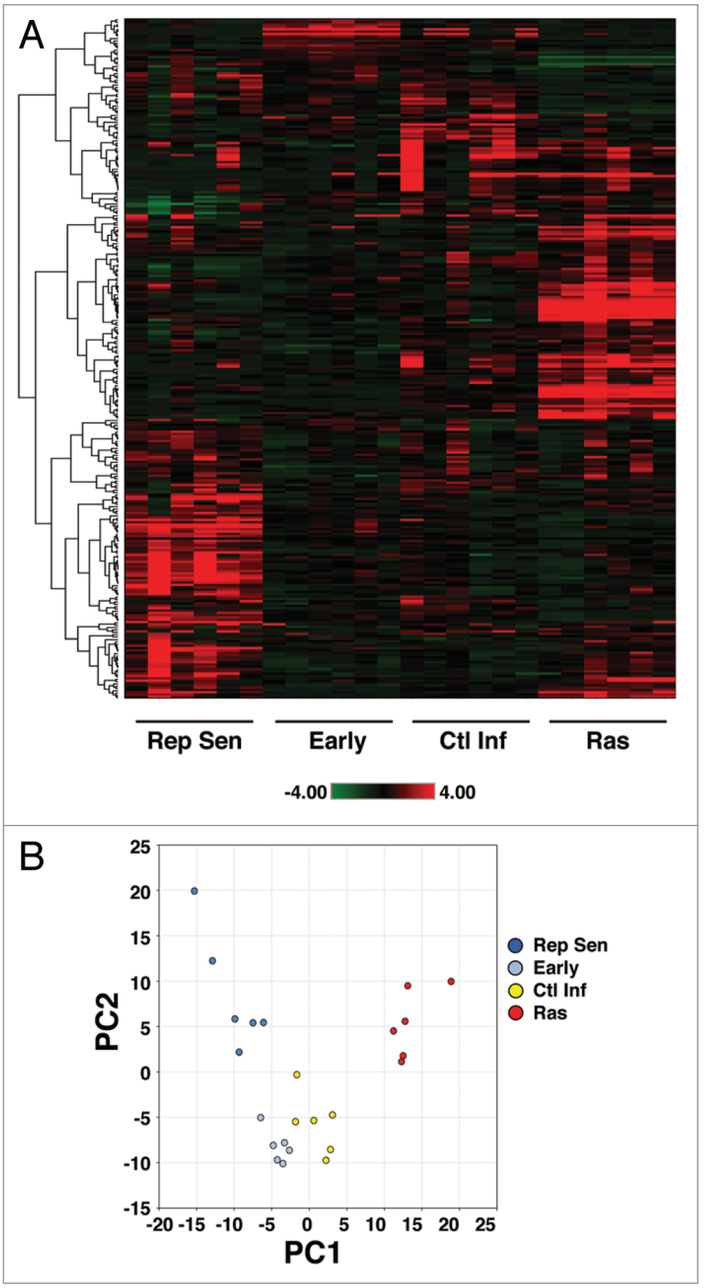

Figure 1. Metabolomic profile of oncogene-induced senescence. (A) Heat map representation of the relative abundance and unsupervised hierarchical clustering of 292 known metabolites in four culture conditions, including early passage uninfected cells (Early), early passage cells infected with a control lentivirus (Ctl Inf), replicative senescent cells (Rep Sen) and Ras-infected senescent cells (Ras). The shade of red or green indicates the relative increase or decrease, respectively, of a particular metabolite relative to the median metabolite levels. Six replicates per condition are shown. (B) Principal component analysis (PCA) of the metabolite data set demonstrating that OIS cells are distinct metabolically. Replicative senescent and Ras-induced senescent cells were distinguishable from each other as well as from non-senescent cells by their projection on principal component 1 (PC1) representing approximately 29% of the variance as well as by their projection on principal component 2 (PC2) representing over 23% of the total variance. The other contributions include PC3 (12%), PC4 (8%) and PC5 (5%).

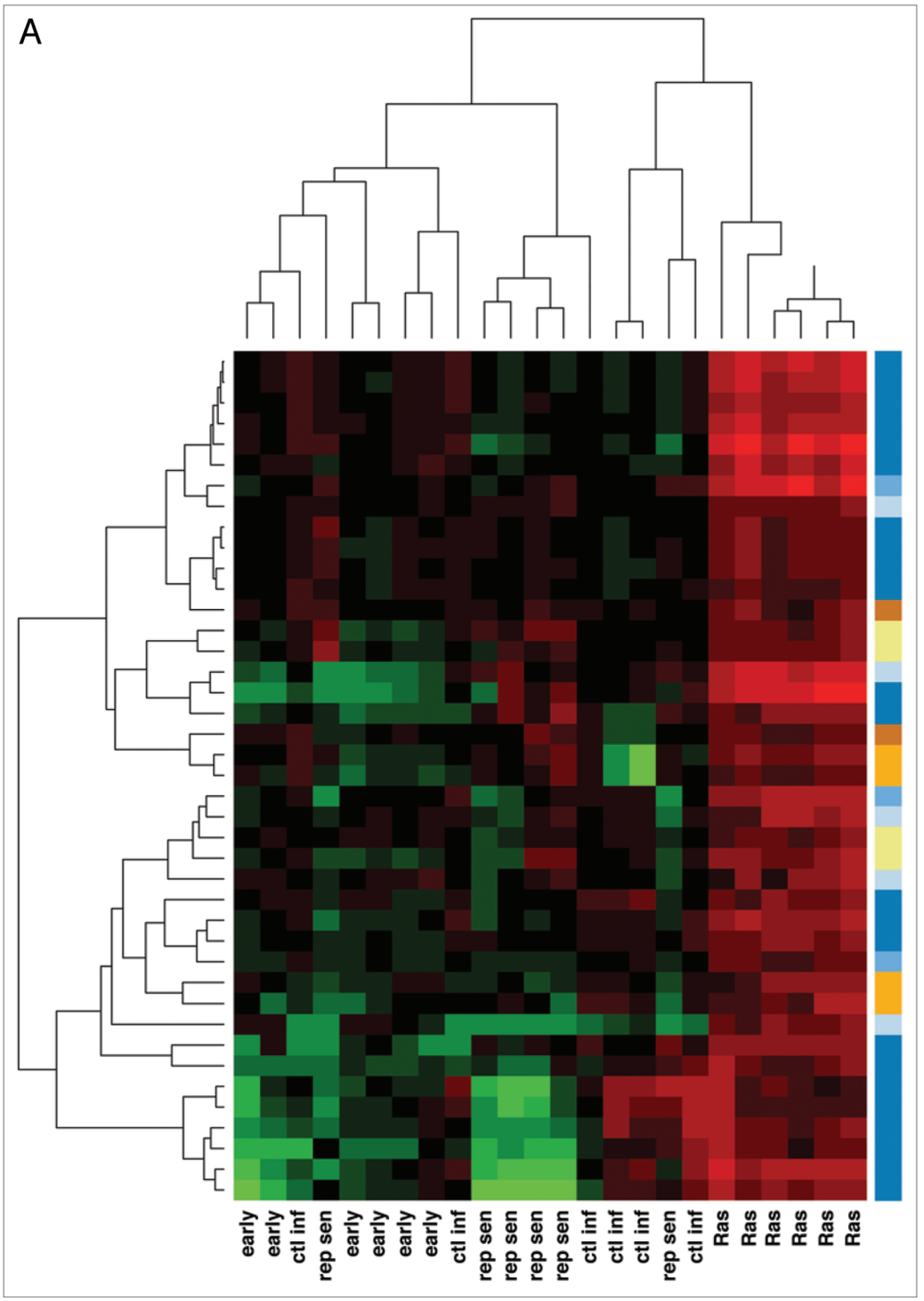

Figure 2A. (A) Ras-induced senescence is accompanied by an alteration in lipid metabolites. (A) Heatmap and unsupervised hierarchal cluster analysis analyzing metabolites uniquely elevated 2-fold or more in OIS cells (n = 6 replicates per condition). Color coded super pathway analysis for these 41 metabolites are denoted in the right hand column.

that have undergone OIS. Reversing the increase in mitochondrial fatty acid oxidation through CPT1A knockdown did not alter Ras-induced growth arrest (**Fig. 4C**), the morphological changes associated with OIS (**Fig. S5**) or the ability of Ras to continuously engage the DDR response (**Fig. 4D**).

We next asked whether restoring a pre-senescent rate of fatty acid oxidation and oxygen consumption might alter the pro-inflammatory, secretory state observed in OIS cells. As expected, when compared with control-infected cells, Ras expression resulted in a 10-fold or greater increase in the levels of various

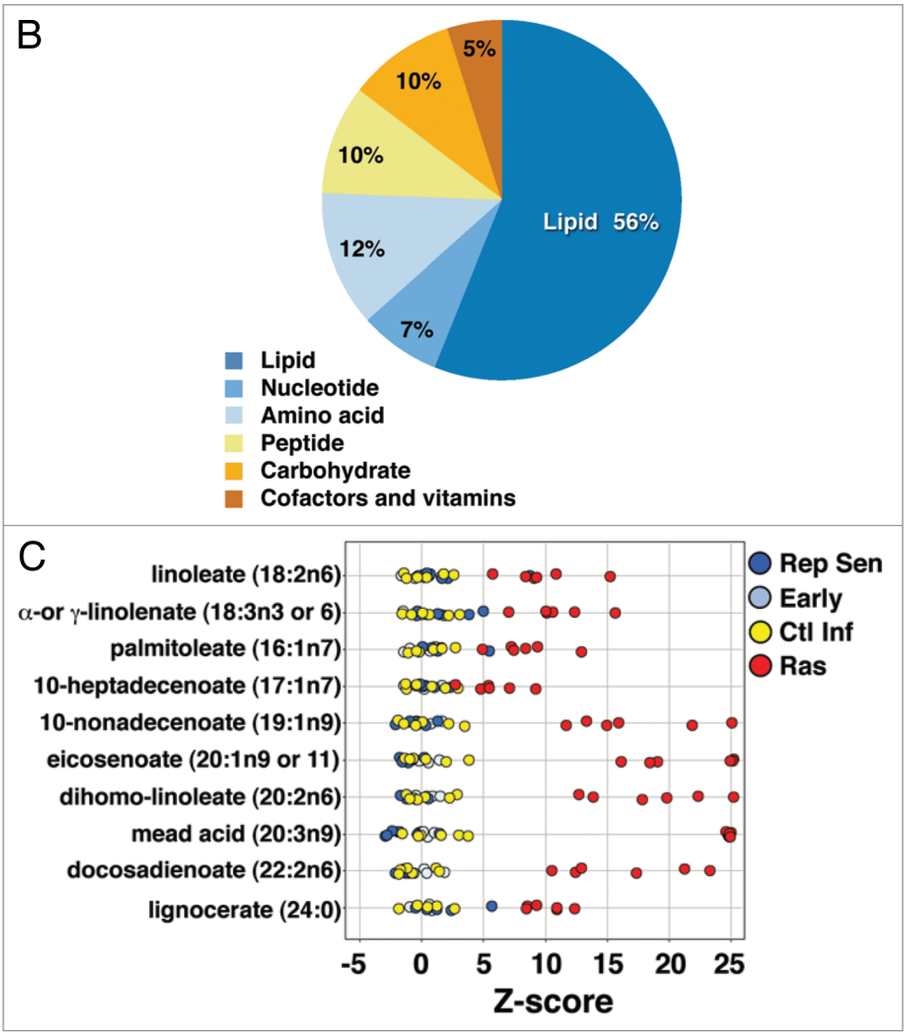

Figure 2B and C. (B and C) Ras-induced senescence is accompanied by an alteration in lipid metabolites. (B) Pathway analysis demonstrates that lipid metabolites are particularly enriched among uniquely elevated biochemicals observed in Ras-infected cells. (C) Z-score plot of some of the specific long chain free fatty acids elevated in the Ras-induced senescent cells (n = 6 replicates per condition).

secreted cytokines (e.g., IL-6 secretion 0.21 ± 0.05 pg per thousand control-infected cells vs. 2.07 ± 0.42 pg per thousand Ras-infected cells, n = 12, $p < 0.001$). This secretory phenotype was not observed in IMR-90 cells undergoing replicative senescence where secretion of various cytokines was either unchanged or actually tended to decrease with passage (e.g., IL-6 secretion 0.09 ± 0.02 pg per thousand uninfected early passage cells vs. 0.04 ± 0.01 pg per thousand replicative senescent cells, n = 3, $p = 0.09$). This lack of a pronounced secretory response in IMR-90 cells undergoing replicative senescence in a 20% oxygen environment has been noted previously in reference 10. Remarkably, acute pharmacological inhibition of CPT1 activity with Etomoxir produced inhibition of a wide array of inflammatory mediators in Ras-induced senescent cells (**Fig. 4E**). The one exception to this Etomoxir-induced cytokine inhibition was secretion of IL-1β, which appeared unaffected by pharmacological inhibition of fatty acid metabolism. Similar results were obtained when OIS cells were subjected to CPT1A knockdown (**Fig. 4F**). Again, with the exception of IL-1β, each of the two independent shRNAs targeting CPT1A resulted in a significant reduction of Ras-induced cytokine production.

Discussion

In summary, we have characterized the metabolic and bioenergetic alterations that occur in Ras-induced senescence. Our data suggests that the metabolic profile of cells undergoing OIS is markedly distinct from cells that undergo replicative senescence. This is a somewhat unexpected finding, since in the past, all senescent cells have been viewed as equivalent. Nonetheless, metabolic profiling appears to provide an ability to resolve distinct forms of senescence depending on the initial trigger, and suggests that senescence may consist of more than one biological state. One of the most striking and unique metabolic characteristic of Ras-induced senescent cells are the marked alterations in intracellular long chain fatty acids. The steady-state levels of

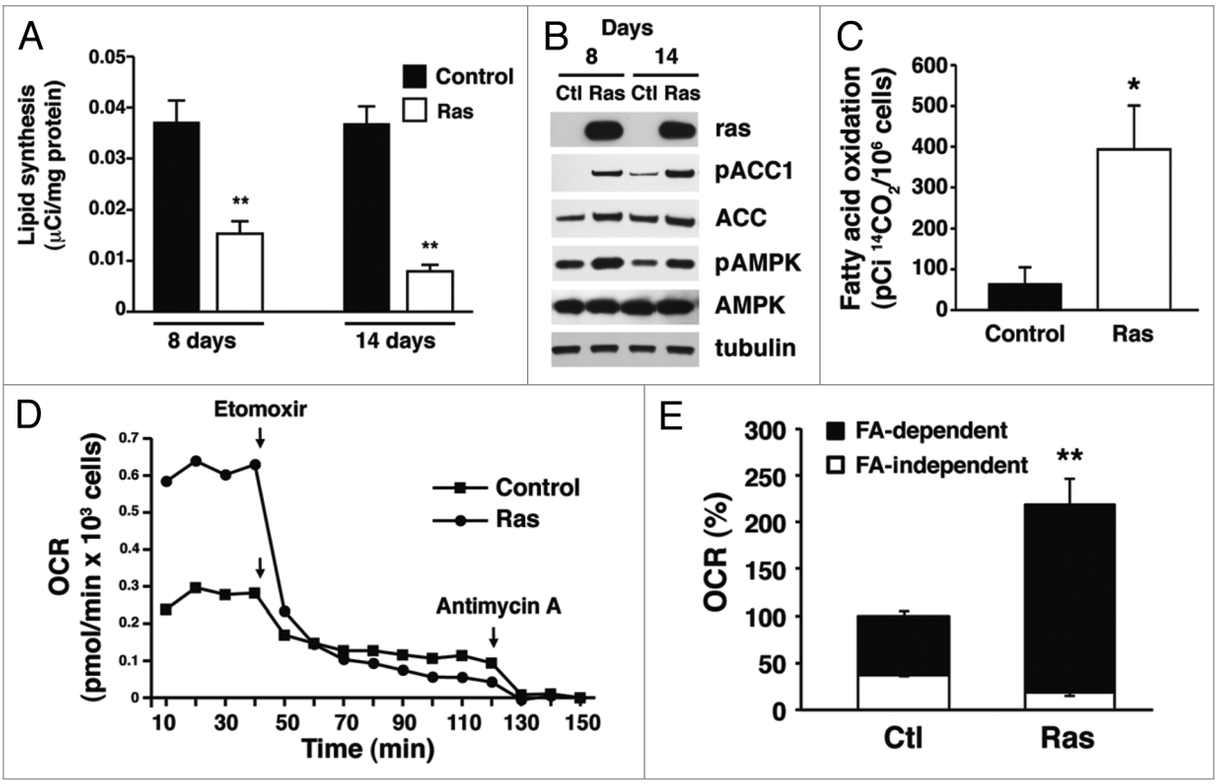

Figure 3. Cells undergoing Ras-mediated senescence exhibit alterations in lipid metabolism. (A) Rates of lipid synthesis as determined by ^{14}C-acetate incorporation in confluent arrested control-infected cells or Ras-infected senescent human fibroblasts either 8 or 14 d after lentivirus infection. (B) Biochemical evidence of ACC inactivation as evidenced by increased serine 79 phosphorylation (pACC1). Serine 79 phosphorylation results in inactivation of the ACC enzyme with a subsequent decrease in lipid synthesis. This ACC1 phosphorylation is catalyzed by AMPK, a kinase that is activated in Ras-induced senescent cells (pAMPK). (C) Fatty acid oxidation as determined by ^{14}C-oleate oxidation to $^{14}CO_2$ is increased in Ras-infected cells. (D) Oxygen consumption rate (OCR) for confluent-arrested control-infected cells or for Ras-infected senescent cells. An approximate 2-fold increase in basal metabolism was observed in Ras-infected cells. Treatment with the CPT1 inhibitor Etomoxir (100 μM) abrogated the differences in oxygen consumption between Ras and control-infected cells. Treatment with the Complex III inhibitor Antimycin A (2.5 μM) reduced oxygen consumption to near zero, suggesting the measured OCR is mitochondrial in origin. (E) Relative oxygen consumption along with the ratio of fatty acid dependent (Etomoxir-sensitive) and fatty acid independent (Etomoxir-insensitive) respiration in control-infected and Ras-infected cells (respiration is normalized to control infected cells). n > 3 replicates per condition for all experiments, *p < 0.05 and **p < 0.01, error bars stand for SE.

metabolites as measured in our metabolomics screen do not provide an assessment of the flux of metabolites through any specific pathway. Indeed the increase in free fatty acids does not appear to reflect an increase in de novo synthesis of fatty acids, as the rates of lipid synthesis were in fact significantly reduced in OIS cells. As such, to extend our observations regarding alterations in the levels of certain free fatty acids, we sought to directly measure the rate of fatty acid oxidation. These experiments demonstrated that mitochondrial oxygen consumption and, in particular, rates of fatty acid oxidation were elevated in Ras-induced senescent cells.

Our observations are more consistent with past observations, where some of the long chain fatty acids identified in our metabolomic screen have been previously implicated as important sources of mitochondrial oxidation and subsequent energy production.[29-32] Consistent with this notion, rates of mitochondrial oxygen consumption and, in particular, rates of fatty acid oxidation were elevated in Ras-induced senescent cells. In this context, it is interesting to note that several recent reports have suggested that alterations in free fatty acid levels and oxidation might modulate the aggressiveness of certain tumors.[33,34] Furthermore, given the connection between senescence and aging, it is also important to note that recent observations also suggest that levels of FFA and certain phospholipid-derived molecules may be important determinants of longevity of simple organisms.[35,36]

Our data also suggests that blocking the senescent-associated increase in mitochondrial fatty acid oxidation can selectively inhibit the secretory state that is associated with OIS. We observed high levels of cytokine production in IMR-90 cells that had undergone Ras-mediated senescence but not in replicative senescent IMR-90 cells. The latter observations are consistent with previous results for this cell line.[10] Further studies will be useful to assess how general the relationship is between fatty acid oxidation and senescence-associated inflammation. Interestingly, in our Ras-infected cells, only IL-1β secretion appeared to be unaffected by genetic or pharmacological inhibition of CPT1A. Among the cytokines tested, secretion of IL-1β is unique, as it occurs through a specific molecular platform termed the inflammasome.[37] Recent evidence suggests a role for mitochondrial ROS in this process.[38-40] These observations, along with the data presented here, would suggest that mitochondrial activity plays a

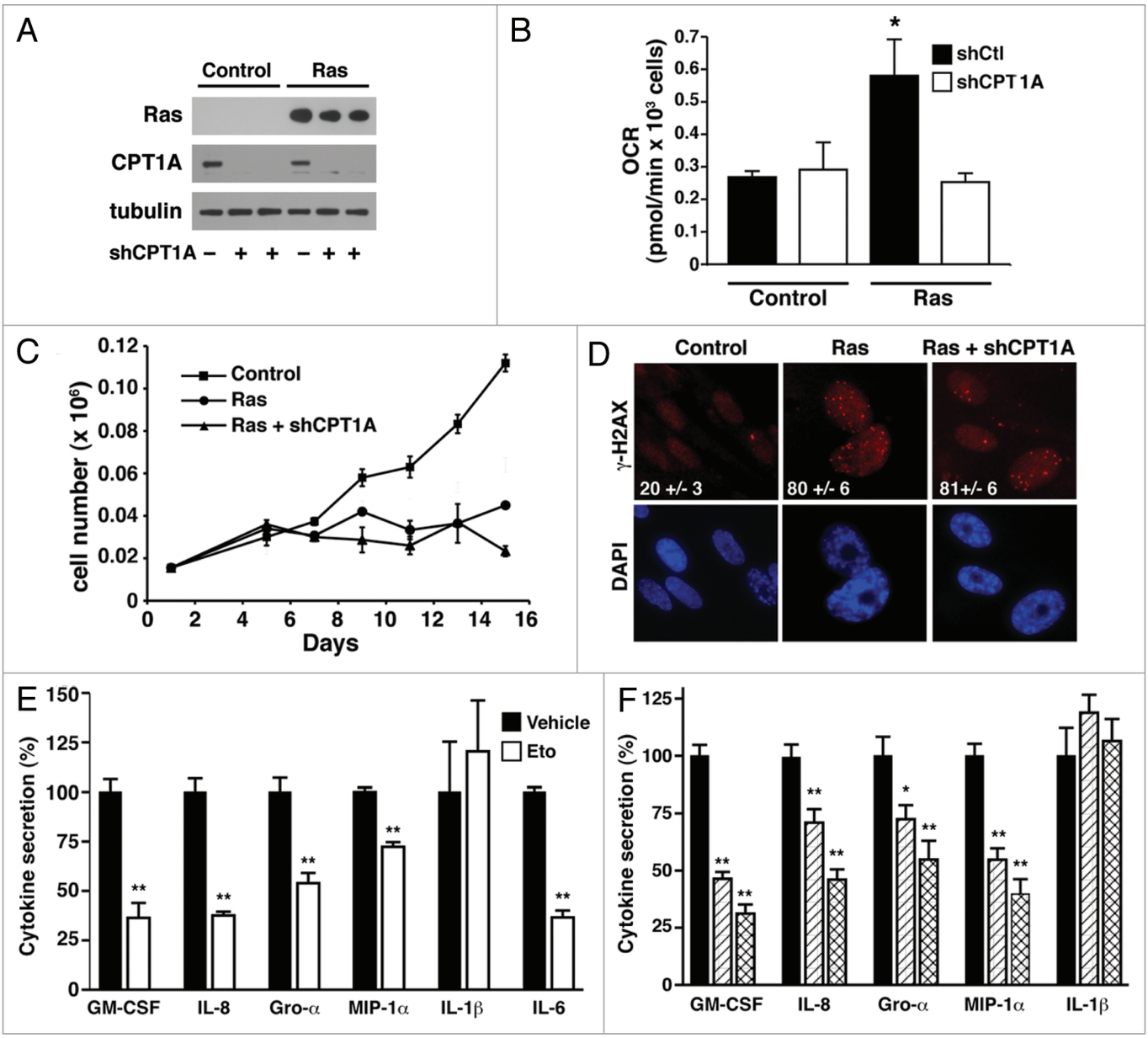

Figure 4. Fatty acid oxidation regulates the secretory state of Ras-induced senescence. (A) Expression of CPT1A in control-infected or Ras-infected cells following knockdown with a control vector (-) or one of two independent shRNAs directed at CPT1A. (B) Knockdown of CPT1A reduces oxygen consumption in Ras-infected cells, consistent with the role of increased fatty acid oxidation in OIS cells. (C) Knockdown of CPT1A does not alter Ras-mediated growth arrest. (D) CPT1A knockdown does not alter Ras-induced activation of the DDR as assessed by γH2AX staining. The percentage of cells with positive nuclei foci is shown in white. (E) Relative levels of cytokine secretion in Ras-infected cells treated with vehicle (filled bars) or for six hours with the CPT1 inhibitor Etomoxir (open bars). (F) Normalized levels of secreted cytokines in Ras-infected cells with a scrambled control shRNA (filled bar) or Ras-infected cells using either of two different shRNAs directed at CPT1A (single and double hatched bars). n > 3 replicates per condition for all experiments, *p < 0.05 and **p < 0.01.

wider role in the maintenance of the inflammatory state than had previously been assumed.

Induction of senescence is thought to play a major beneficial role in tumor suppression.[2,15,41] In contrast, accumulation of pro-inflammatory senescent cells is thought to contribute to various detrimental aspects of the aging process.[11,16,42] Consistent with this notion, normal human aging is accompanied by a rise in circulating inflammatory cytokines, and the degree of activation of this inflammatory program inversely correlates with longevity and freedom from various age-associated pathologies.[17-19] Thus, while the induction of senescent growth arrest, DDR engagement and inflammation are intimately connected,[43] our results suggest that specific metabolic interventions can effectively decouple these events. Strategies that inhibit fatty acid oxidation might therefore reduce the harmful inflammatory profile associated with OIS senescence without inhibiting the beneficial

growth arrest and tumor suppressor functions. As such, these metabolic approaches might be an effective strategy to reduce the severity of various age-related pathologies without substantially increasing the predisposition for cancer.

Materials and Methods

Cell culture and replicative senescent cells. IMR-90 cells were cultured weekly using an initial seeding density of 0.5 x 10^6 cells per 10 cm dish. These cells were routinely grown in Dulbecco's modified Eagle's medium (DMEM, Invitrogen) with low glucose (1 mg/ml) supplemented with 10% (v/v) fetal bovine serum (FBS), penicillin 50 U/ml and streptomycin 50 ug/ml. Cells were maintained at 37°C in a CO_2 incubator (95% air, 5% CO_2). Under our experimental conditions, IMR-90 cultures entered replicative senescence (Rep Sen) after achieving a PDL value of approximately 50. At this point, fibroblasts could not reach confluence after 7–10 d following a 1:2 split, and 60–80% of the cells routinely stained positive for senescence associated β-galactosidase (SA-β-Gal). Cells with PDL between 25–36 were denominated early passage cells (early: <2% of the cells routinely stained positive for SA-β-Gal). For growth curves, 1.4 x 10^4 cells were initially plated per well of a 12-well plates. At the indicated times, cells were detached using Tryple express, and live cell number was assessed using a Countess Automated Cell Counter (Invitrogen) and trypan blue (Invitrogen).

Lentiviral shRNA transduction. Lentiviral shRNA constructs targeting CPT1A were purchased from Sigma-Aldrich (shCPT1A ID TRCN0000036282 and TRCN0000036283). The lentiviral plasmid expressing H-Ras containing a glycine to valine substitution at position 12 was obtained from Addgene. The control plasmid was from Open Biosystems. Lentivirus constructs were amplified in 293T cells according to protocols established by the Broad Institute RNAi Consortium (www.broadinstitute.org/genome_bio/trc/publicProtocols.html). For infection, one to two days after seeding, early passage IMR-90 cells were transduced with lentiviruses (MOI of 1–5) overnight in media containing 8 μg/ml polybrene. Infected cells were subsequently selected in culture media supplemented with 2 μg/ml puromycin (Sigma-Aldrich).

Generation of oncogene induced senescent cells. Early passage IMR-90 cells were infected with H-RAS containing lentivirus (Ras) or a lentivirus containing a control plasmid (Ctl). One week after infection with RAS containing lentivirus, cells manifested an arrest in proliferation. Two weeks after infection, 60–80% of the cells stained positive for senescence associated β-galactosidase (SA-β-Gal) and exhibited evidence for activation of the DNA damage response (DDR) (**Fig. S1**). Unless otherwise specified, all experiments regarding Ras-induced senescence where performed 14 d after infection.

Metabolomics. Samples were split for separate analysis on the GC/MS and LC/MS/MS platforms. All cell line treatment, metabolite analysis, sample preparation, quality assurance procedures, spectroscopy as well as statistical analysis was performed as previously described in reference 44. Raw data was normalized to Bradford protein content prior to statistical analysis. The data set comprises a total 292 named biochemicals. Following log transformation and imputation with minimum observed values for each compound, Welch's two-sample t-test was used to identify biochemicals that differed significantly between any pair of the four specific conditions. The False Discovery Rate (FDR) for a given set of compounds was estimated using the q-value[45] in order to take into account the multiple comparisons that normally occur in metabolomic-based studies; as q-values were reasonable for $p \leq 0.05$, no q-value cutoff was established for this study.

Hierarchical clustering and PCA plots were generated in Array Studio (Omicsoft Corporation) version 4.0.0.6 and using the g-plots package (CRAN.R-project.org/package=gplots) for R version 2.12 (www.R-project.org). Hierarchical clustering was generated using the correlation-based distance between samples and complete linkage algorithm.

Lipid synthesis. Lipid biosynthesis was assessed as previously described using the incorporation of [^{14}C]-acetate into cell lipids.[46] Control-infected or Ras-infected cells were seeded onto 60 mm dishes, and on the day of the experiment, cells were washed with PBS and then incubated for 2 h in 2 ml of DMEM supplemented with 4.5 g/l D-glucose and 0.1% FBS. Acetic acid [2-^{14}C] sodium salt (1 μCi, Perkin Elmer) was added to the cells for a 3-h pulse, after which the cells were washed with PBS, harvested using 600 μl of Tryple express (Invitrogen) dissociation buffer, centrifuged and washed again with PBS. Organic extraction of the cell lipids was performed as previously described in reference 47. Radioactivity was determined in the incubation media, aqueous phase and organic phase using a liquid scintillation counter. To control for differences in proliferation, the experiments were performed with confluent-arrested control-infected cells or senescent, non-proliferating Ras-infected cells.

Oxygen consumption rate. Oxygen consumption rate (OCR) was measured at 37°C using an XF24 extracellular analyzer (Seahorse Bioscience) as previously described in reference 48. Briefly, cells were initially changed to unbuffered DMEM (DMEM with 5 mM glucose, 1 mM sodium pyruvate, 32 mM NaCl, 2 mM GlutaMax, pH 7.4) and incubated in a non-CO_2 incubator for 2 h at 37°C. Four baseline measurements were taken before injection of mitochondrial inhibitors or uncouplers. Readings were taken after sequential addition of Etomoxir (100 μM) and antimycin A (0.5 μM) or oligomycin (0.5 uM), carbonyl cyanide 4-(trifluoromethoxy)phenylhydrazone (FCCP, 0.25 μM) and antimycin A. Oxygen consumption rates were calculated by the Seahorse XF-24 software and represent an average of 3–6 different samples. After the assays, cell number was determined in each well using a Coulter counter (Beckman) and the rate of measured oxygen consumption was normalized to cell number. Antimycin-resistant respiration was subtracted from all measurements in order to analyze mitochondrial oxygen consumption. All the oxygen consumption studies were performed with confluent-arrested control cells or non-proliferating senescent cells.

Fatty acid conjugation. To conjugate the free fatty acid oleate to BSA, we initially prepared 100 mM sodium oleate (Sigma-Aldrich) by mixing 47.5 mg of oleate in 1.5 ml of water with 2.5 μl of 1 N NaOH. The solution was heated to 37°C and vortexed occasionally until dissolved. Sodium oleate was then mixed

with a solution of fatty acid free BSA (Sigma) dissolved in PBS (15% weight to volume). The resulting mixture was then incubated for 30 min at 42°C to obtain an oleate:BSA stock solution (7 mM:14%). To incorporate radioactive oleate to FFA:BSA, [1-^{14}C] oleic acid (0.1 mCi, American Radiolabeled Chemicals) was dried under vacuum and resuspended in 1 ml of oleate: BSA (1 mM: 2%) in PBS and incubated under agitation at 60°C for 2 h.

Fatty acid oxidation. IMR-90 fibroblasts were seeded in 24-well plates and fatty acid oxidation assessed 14 d after infection with either the control or Ras lentiviruses. The day of the experiment, cells were washed with PBS and incubated in serum-free media for 1.5 h. Media was then removed and substituted with 0.95 ml of preincubation media (DMEM with 25 mM Hepes with oleate:BSA at 0.1 mM:0.2%) in the presence or absence of 1 mM Etomoxir (Sigma) as previously described in reference 49. After 1 h, 50 μl of labeled [1-^{14}C] oleate:oleate:BSA was added to the cells. After an additional 90 min, 400 μl of media was transferred to collection tubes consisting of polypropylene eppendorfs with 200 μl of perchloric acid (1 M) and a filter paper embedded in 30 μl of 3 M NaOH contained within the cap. The tubes were closed and [^{14}C] CO_2 collected for 1.5 h at room temperature. Following this collection period, the filter paper was transferred to a scintillation vial, and 3 ml of scintillation fluid were added. Scintillation counts were determined 24 h later after strong vortexing of each sample for 1 min. Background was determined by performing a similar analysis using cells with no labeled substrate. To control for differences in proliferation, the experiments were performed with confluent-arrested control-infected cells or senescent, non-proliferating Ras-infected cells.

SAβ-Gal staining and DDR assessment. SA-β-Gal analysis of fibroblasts was determined as previously described in reference 50 using the Senescence β-Galactosidase Staining Kit (Cell Signaling Technology Inc.). The percentage of positive staining was calculated by counting > 100 cell in five different fields. Three different wells were analyzed per condition, and results are expressed as the mean ± SE.

The activation of the DNA damage response (DDR) was assessed by analysis of γH2AX foci. Cells were cultured on chamber slides that were first fixed with 4% paraformaldehyde in PBS for 10 min and then permeabilized for an additional 10 min with 0.2% Triton X-100 in PBS. After permeabilization, cells were incubated for 1 h in blocking buffer composed of 0.2% Triton X-100 and 3% BSA in PBS followed by incubation overnight at 4°C with the primary antibody [γH2AX (S139) Millipore, 1:2,000]. The following day, slides were incubated with a rhodamine (TRITC)-conjugated goat anti-rabbit IgG secondary antibody (Jackson Immunoresearch, 1:1,000). The percentage positive staining was calculated by counting foci formation in > 100 random nuclei in five different fields. Three different chamber slides were analyzed per condition; results are expressed as the mean ± SE.

Protein expression analysis. For protein expression, cells were routinely lysed in Cell Lysis Buffer (Cell Signaling Technology) containing 20 mM Tris, pH 7.4, 1% Triton X-100, 20 mM TRIS-HCl (pH 7.5), 150 mM NaCl, 1 mM EDTA, 1 mM EGTA, 2.5 mM sodium pyrophosphate, 1 mM β-glycerophosphate, 1 mM Na_2VO_4 and Halt protease and phosphatase inhibitor cocktail (Thermo Scientific). Lysates were sonicated, centrifuged at 14,000 g for 10 min and stored at -80°C. Proteins were resolved by SDS-PAGE and subjected to western blotting using standard procedures. The following primary antibodies were used: acetyl-CoA carboxylase, phospho-ACC1 (Ser 79), AMPK, phospho-AMPK (Thr 172) and Ras (Cell Signaling); α-tubulin (Santa Cruz Biotechnology); CPT1A (Sigma).

Cytokine assays. IMR-90 fibroblasts (2 x 10^4 cells) were plated in 24-well dishes and transduced with either the control or Ras lentivirus. Where indicated, cells were also infected with one of the two shRNAs directed against CPT1A. Fourteen days later, cells were washed with PBS and 500 μl of serum free DMEM was added to the culture. In some experiments, this final incubation also contained Etomoxir (1 mM) or the vehicle control. After 6 h, the media was collected, centrifuged at 14,000 g to remove cells and debris and subsequently stored at -80°C for later analysis. GM-CSF, MIP-1α, GROα, IL-8, IL-6 and IL-1β cytokine analysis were performed by ELISA using DuoSet ELISA kits (R&D Systems). Results were normalized to cell number, as determined after detaching the cells and counting with a Beckman Coulter cell and particle counter. Results are pooled from between 2–4 similar experiments (n = 3–12 replicates per condition). As previously noted, for the cytokines tested, Ras infection led to a large increase in cytokine production.[10] In contrast, cytokine levels in control infected cells were at or near the limit of detection.

Disclosure of Potential Conflicts of Interest

No potential conflicts of interest were disclosed.

Acknowledgments

This work was supported by NIH Intramural funds.

Note

Supplemental material can be found at:
www.landesbioscience.com/journals/cc/article/19800

References

1. Hayflick L. Limited in Vitro Lifetime of Human Diploid Cell Strains. Exp Cell Res 1965; 37:614-36; PMID:14315085; http://dx.doi.org/10.1016/0014-4827(65)90211-9.
2. Collado M, Blasco MA, Serrano M. Cellular senescence in cancer and aging. Cell 2007; 130:223-33; PMID:17662938; http://dx.doi.org/10.1016/j.cell.2007.07.003.
3. Shay JW, Wright WE. Telomeres and telomerase in normal and cancer stem cells. FEBS Lett 2010; 584:3819-25; PMID:20493857; http://dx.doi.org/10.1016/j.febslet.2010.05.026.
4. d'Adda di Fagagna F, Reaper PM, Clay-Farrace L, Fiegler H, Carr P, Von Zglinicki T, et al. A DNA damage checkpoint response in telomere-initiated senescence. Nature 2003; 426:194-8; PMID:14608368; http://dx.doi.org/10.1038/nature02118.
5. Serrano M, Lin AW, McCurrach ME, Beach D, Lowe SW. Oncogenic ras provokes premature cell senescence associated with accumulation of p53 and p16^{INK4a}. Cell 1997; 88:593-602; PMID:9054499; http://dx.doi.org/10.1016/S0092-8674(00)81902-9.
6. Collado M, Gil J, Efeyan A, Guerra C, Schuhmacher AJ, Barradas M, et al. Tumour biology: senescence in premalignant tumours. Nature 2005; 436:642; PMID:16079833; http://dx.doi.org/10.1038/436642a.

7. Braig M, Lee S, Loddenkemper C, Rudolph C, Peters AH, Schlegelberger B, et al. Oncogene-induced senescence as an initial barrier in lymphoma development. Nature 2005; 436:660-5; PMID:16079837; http://dx.doi.org/10.1038/nature03841.
8. Michaloglou C, Vredeveld LC, Soengas MS, Denoyelle C, Kuilman T, van der Horst CM, et al. $BRAF_{E600}$-associated senescence-like cell cycle arrest of human naevi. Nature 2005; 436:720-4; PMID:16079850; http://dx.doi.org/10.1038/nature03890.
9. Chen Z, Trotman LC, Shaffer D, Lin HK, Dotan ZA, Niki M, et al. Crucial role of p53-dependent cellular senescence in suppression of Pten-deficient tumorigenesis. Nature 2005; 436:725-30; PMID:16079851; http://dx.doi.org/10.1038/nature03918.
10. Coppé JP, Patil CK, Rodier F, Sun Y, Muñoz DP, Goldstein J, et al. Senescence-associated secretory phenotypes reveal cell-nonautonomous functions of oncogenic RAS and the p53 tumor suppressor. PLoS Biol 2008; 6:2853-68; PMID:19053174; http://dx.doi.org/10.1371/journal.pbio.0060301.
11. Rodier F, Campisi J. Four faces of cellular senescence. J Cell Biol 2011; 192:547-56; PMID:21321098; http://dx.doi.org/10.1083/jcb.201009094.
12. Wajapeyee N, Serra RW, Zhu X, Mahalingam M, Green MR. Oncogenic BRAF induces senescence and apoptosis through pathways mediated by the secreted protein IGFBP7. Cell 2008; 132:363-74; PMID:18267069; http://dx.doi.org/10.1016/j.cell.2007.12.032.
13. Kuilman T, Michaloglou C, Vredeveld LC, Douma S, van Doorn R, Desmet CJ, et al. Oncogene-induced senescence relayed by an interleukin-dependent inflammatory network. Cell 2008; 133:1019-31; PMID:18555778; http://dx.doi.org/10.1016/j.cell.2008.03.039.
14. Acosta JC, O'Loghlen A, Banito A, Guijarro MV, Augert A, Raguz S, et al. Chemokine signaling via the CXCR2 receptor reinforces senescence. Cell 2008; 133:1006-18; PMID:18555777; http://dx.doi.org/10.1016/j.cell.2008.03.038.
15. Gorgoulis VG, Halazonetis TD. Oncogene-induced senescence: the bright and dark side of the response. Curr Opin Cell Biol 2010; 22:816-27; PMID:20807678; http://dx.doi.org/10.1016/j.ceb.2010.07.013.
16. Campisi J. Cellular senescence: putting the paradoxes in perspective. Curr Opin Genet Dev 2011; 21:107-12; PMID:21093253; http://dx.doi.org/10.1016/j.gde.2010.10.005.
17. Bruunsgaard H, Andersen-Ranberg K, Hjelmborg JB, Pedersen BK, Jeune B. Elevated levels of tumor necrosis factoralpha and mortality in centenarians. Am J Med 2003; 115:278-83; PMID:12967692; http://dx.doi.org/10.1016/S0002-9343(03)00329-2.
18. Ferrucci L, Harris TB, Guralnik JM, Tracy RP, Corti MC, Cohen HJ, et al. Serum IL-6 level and the development of disability in older persons. J Am Geriatr Soc 1999; 47:639-46; PMID:10366160.
19. Alley DE, Crimmins E, Bandeen-Roche K, Guralnik J, Ferrucci L. Three-year change in inflammatory markers in elderly people and mortality: the Invecchiare in Chianti study. J Am Geriatr Soc 2007; 55:1801-7; PMID:17727645; http://dx.doi.org/10.1111/j.1532-5415.2007.01390.x.
20. Zwerschke W, Mazurek S, Stöckl P, Hütter E, Eigenbrodt E, Jansen-Dürr P. Metabolic analysis of senescent human fibroblasts reveals a role for AMP in cellular senescence. Biochem J 2003; 376:403-11; PMID:12943534; http://dx.doi.org/10.1042/BJ20030816.
21. Kondoh H, Lleonart ME, Gil J, Wang J, Degan P, Peters G, et al. Glycolytic enzymes can modulate cellular life span. Cancer Res 2005; 65:177-85; PMID:15665293.
22. Lipetz J, Cristofalo VJ. Ultrastructural changes accompanying the aging of human diploid cells in culture. J Ultrastruct Res 1972; 39:43-56; PMID:5017037; http://dx.doi.org/10.1016/S0022-5320(72)80005-4.
23. Kim YM, Shin HT, Seo YH, Byun HO, Yoon SH, Lee IK, et al. Sterol regulatory element-binding protein (SREBP)-1-mediated lipogenesis is involved in cell senescence. J Biol Chem 2010; 285:29069-77; PMID:20615871; http://dx.doi.org/10.1074/jbc.M110.120386.
24. Lee AC, Fenster BE, Ito H, Takeda K, Bae NS, Hirai T, et al. Ras proteins induce senescence by altering the intracellular levels of reactive oxygen species. J Biol Chem 1999; 274:7936-40; PMID:10075689; http://dx.doi.org/10.1074/jbc.274.12.7936.
25. Passos JF, Saretzki G, Ahmed S, Nelson G, Richter T, Peters H, et al. Mitochondrial dysfunction accounts for the stochastic heterogeneity in telomere-dependent senescence. PLoS Biol 2007; 5:110; PMID:17472436; http://dx.doi.org/10.1371/journal.pbio.0050110.
26. Moiseeva O, Bourdeau V, Roux A, Deschênes-Simard X, Ferbeyre G. Mitochondrial dysfunction contributes to oncogene-induced senescence. Mol Cell Biol 2009; 29:4495-507; PMID:19528227; http://dx.doi.org/10.1128/MCB.01868-08.
27. Carling D, Clarke PR, Zammit VA, Hardie DG. Purification and characterization of the AMP-activated protein kinase. Copurification of acetyl-CoA carboxylase kinase and 3-hydroxy-3-methylglutaryl-CoA reductase kinase activities. Eur J Biochem 1989; 186:129-36; PMID:2598924; http://dx.doi.org/10.1111/j.1432-033.1989.tb15186.x.
28. Tong L. Acetyl-coenzyme A carboxylase: crucial metabolic enzyme and attractive target for drug discovery. Cell Mol Life Sci 2005; 62:1784-803; PMID:15968460; http://dx.doi.org/10.1007/s00018-005-5121-4.
29. Demizieux L, Degrace P, Gresti J, Loreau O, Noël JP, Chardigny JM, et al. Conjugated linoleic acid isomers in mitochondria: evidence for an alteration of fatty acid oxidation. J Lipid Res 2002; 43:2112-22; PMID:12454273; http://dx.doi.org/10.1194/jlr.M200170-JLR200.
30. Burdge G. Alpha-linolenic acid metabolism in men and women: nutritional and biological implications. Curr Opin Clin Nutr Metab Care 2004; 7:137-44; PMID:15075703; http://dx.doi.org/10.1097/00075197-200403000-00006.
31. Bremer J, Norum KR. Metabolism of very long-chain monounsaturated fatty acids (22:1) and the adaptation to their presence in the diet. J Lipid Res 1982; 23:243-56; PMID:7042878.
32. Cunnane SC, Ross R, Bannister JL, Jenkins DJ. Beta-oxidation of linoleate in obese men undergoing weight loss. Am J Clin Nutr 2001; 73:709-14; PMID:11273844.
33. Nomura DK, Long JZ, Niessen S, Hoover HS, Ng SW, Cravatt BF. Monoacylglycerol lipase regulates a fatty acid network that promotes cancer pathogenesis. Cell 2010; 140:49-61; PMID:20079333; http://dx.doi.org/10.1016/j.cell.2009.11.027.
34. Zaugg K, Yao Y, Reilly PT, Kannan K, Kiarash R, Mason J, et al. Carnitine palmitoyltransferase 1C promotes cell survival and tumor growth under conditions of metabolic stress. Genes Dev 2011; 25:1041-51; PMID:21576264; http://dx.doi.org/10.1101/gad.1987211.
35. Shmookler Reis RJ, Xu LL, Lee H, Chae M, Thaden JJ, Bharill P, et al. Modulation of lipid biosynthesis contributes to stress resistance and longevity of *C. elegans* mutants. Aging (Albany NY) 2011; 3:125-47; PMID:21386131.
36. Lucanic M, Held JM, Vantipalli MC, Klang IM, Graham JB, Gibson BW, et al. N-acylethanolamine signalling mediates the effect of diet on lifespan in *Caenorhabditis elegans*. Nature 2011; 473:226-9; PMID:21562563; http://dx.doi.org/10.1038/nature10007.
37. Schroder K, Tschopp J. The inflammasomes. Cell 2010; 140:821-32; PMID:20303873; http://dx.doi.org/10.1016/j.cell.2010.01.040.
38. Bulua AC, Simon A, Maddipati R, Pelletier M, Park H, Kim KY, et al. Mitochondrial reactive oxygen species promote production of proinflammatory cytokines and are elevated in TNFR1-associated periodic syndrome (TRAPS). J Exp Med 2011; 208:519-33; PMID:21282379; http://dx.doi.org/10.1084/jem.20102049.
39. Nakahira K, Haspel JA, Rathinam VA, Lee SJ, Dolinay T, Lam HC, et al. Autophagy proteins regulate innate immune responses by inhibiting the release of mitochondrial DNA mediated by the NALP3 inflammasome. Nat Immunol 2011; 12:222-30; PMID:21151103; http://dx.doi.org/10.1038/ni.1980.
40. Zhou R, Yazdi AS, Menu P, Tschopp J. A role for mitochondria in NLRP3 inflammasome activation. Nature 2011; 469:221-5; PMID:21124315; http://dx.doi.org/10.1038/nature09663.
41. Kuilman T, Michaloglou C, Mooi WJ, Peeper DS. The essence of senescence. Genes Dev 2010; 24:2463-79; PMID:21078816; http://dx.doi.org/10.1101/gad.1971610.
42. Kuilman T, Peeper DS. Senescence-messaging secretome: SMS-ing cellular stress. Nat Rev Cancer 2009; 9:81-94; PMID:19132009; http://dx.doi.org/10.1038/nrc2560.
43. Rodier F, Coppé JP, Patil CK, Hoeijmakers WAM, Muñoz DP, Raza SR, et al. Persistent DNA damage signalling triggers senescence-associated inflammatory cytokine secretion. Nat Cell Biol 2009; 11:973-9; PMID:19597488; http://dx.doi.org/10.1038/ncb1909.
44. Reitman ZJ, Jin G, Karoly ED, Spasojevic I, Yang J, Kinzler KW, et al. Profiling the effects of isocitrate dehydrogenase 1 and 2 mutations on the cellular metabolome. Proc Natl Acad Sci USA 2011; 108:3270-5; PMID:21289278; http://dx.doi.org/10.1073/pnas.1019393108.
45. Storey JD, Tibshirani R. Statistical significance for genomewide studies. Proc Natl Acad Sci USA 2003; 100:9440-5; PMID:12883005; http://dx.doi.org/10.1073/pnas.1530509100.
46. Howard BV, Howard WJ, Bailey JM. Acetyl coenzyme A synthetase and the regulation of lipid synthesis from acetate in cultured cells. J Biol Chem 1974; 249:7912-21; PMID:4473453.
47. Bligh EG, Dyer WJ. A rapid method of total lipid extraction and purification. Can J Biochem Physiol 1959; 37:911-7; PMID:13671378; http://dx.doi.org/10.1139/o59-099.
48. Liu J, Cao L, Chen J, Song S, Lee IH, Quijano C, et al. Bmi1 regulates mitochondrial function and the DNA damage response pathway. Nature 2009; 459:387-92; PMID:19404261; http://dx.doi.org/10.1038/nature08040.
49. Mao X, Kikani CK, Riojas RA, Langlais P, Wang L, Ramos FJ, et al. APPL1 binds to adiponectin receptors and mediates adiponectin signalling and function. Nat Cell Biol 2006; 8:516-23; PMID:16622416; http://dx.doi.org/10.1038/ncb1404.
50. Dimri GP, Lee X, Basile G, Acosta M, Scott G, Roskelley C, et al. A biomarker that identifies senescent human cells in culture and in aging skin in vivo. Proc Natl Acad Sci USA 1995; 92:9363-7; PMID:7568133; http://dx.doi.org/10.1073/pnas.92.20.9363.